INTERNATIONAL JOURNAL OF AUTOMOTIVE SCIENCE AND TECHNOLOGY

2023, VOL. 7, NO: 2, 78-86 www.ijastech.org e-ISSN: 2587-0963

Experimental Examination of Recovery by a Thermoelectric Generator of Heat Energy Lost to Engine Coolant in a SI Engine

Habib Gürbüz[1*], Hüsameddin Akçay[1] and Beyza Öztop[1]

0000-0001-5157-6227, 0000-0002-5704-670X, 0000-0002-1542-1284

[1] *Department of Automotive Engineering, Faculty of Engineering, Süleyman Demirel University, 32200, Isparta/Turkey*

Abstract

In this study, the recovery of heat energy lost to the engine coolant (Ec) in a liquid-cooled, gas-fueled (propane), spark ignition (SI) engine using a thermoelectric generator (TEG) is experimentally researched. A two-layer rectangular geometry TEG is designed, consisting of a propane heat exchanger (P_hex) located on the surface of an engine coolant heat exchanger (Ec_hex). 20 items of thermoelectric modules (TEMs), each 30x30 mm in dimensions, are placed between the Ec_hex and P_hex. In the TEG design, engine cooling fluid is used on the hot surface of the TEMs, and pro-pane gas fed to the engine is used on the cold surface. In addition, with the use of the designed TEG, there is no need to use an additional evaporator for propane gas. Experiments are carried out with the designed TEG at 8 engine speeds ranging from 1500 to 5000 rpm. As a result, TEG produces 1.25–3.01 W of DC electrical power in the engine's 1500–5000 rpm range, while TEG efficiency fluctuates between 2.7 and 3.1%. However, the maximum TEG_power is 3.01 W at 5000 rpm, while the maxi-mum TEG_efficiency is 3.1% at 1500 rpm. On the other hand, the electrical power of TEG between 1500 – 5000 rpm of the engine is approximately 1.1–1.26% of the engine charging system power. However, TEG's contribution to the charging system again decreases with the engine speed.

Keywords: SI engine, Liquid Cooling system, Propane, Waste heat recovery, Thermoelectric Generator.

Research Article
https://doi.org/10.30939/ijastech..1248944

Received 08.12.2023
Revised 05.04.2023
Accepted 12.04.2023

*Corresponding author
Habib Gürbüz
habibgurbuz@sdu.edu.tr
Address: Automotive Engineering Department, Faculty of Engineering, Süleyman Demirel University, 32200 Isparta, Turkey
Tel: +90 246 2181 18 67
Fax: +902 46 211 10 72

1. Introduction

The European Sustainable Development Policy 2020 report highlights the need to decrease the usage of fossil-based energy sources, including coal, gas, and oil, in order to establish a low-carbon economy [1]. Therefore, the development of innovative technologies that increase energy efficiency and reduce fossil fuel use has become a very important issue [2]. In vehicles with internal combustion engines (ICEs), which constitute an important part of energy consumption in the transportation sector, an imported part of the fuel energy is lost together with the exhaust gases and engine cooling system. Therefore, the use of waste heat recycling systems in ICE vehicles to improve fuel efficiency is a critical issue [3]. Thermoelectric generators (TEGs), which can produce energy without a moving part, have an important advantage for waste heat energy recycling [4]. In this respect, TEGs using thermoelectric material have great potential to reuse some of the waste energy and reduce the CO_2 emissions released into the atmosphere while increasing fuel efficiency. TEMs convert waste heat directly into electrical energy using semiconductor materials [5, 6]. Therefore, TEG systems have attracted the attention of ICE automotive manufacturers and researchers [7]. However, use of TEM in automotive systems is currently not in demand due to its low energy conversion efficiencies, and research and development studies are still ongoing [8].

When the surfaces of thermoelectric modules (TEMs) used in the structure of TEGs are subjected to a temperature difference of ΔT, they generate electrical potential (voltage and current) through an external electrical circuit. The voltage difference produced in TEMs is proportional to the temperature difference acting on their surfaces. The electrical power that can be produced with TEGs can vary from microwatts to kilowatts depending on the waste heat system to which it is applied [9]. In systems where more than a few watts are required, a series and/or parallel group of multiple TEMs can be used to produce the required power level. The required voltage and/or current in TEGs are obtained generally through these connecting methods [10]. Today, the focus is on using many engine components to increase the effectiveness of TEGs developed to recover wasted fuel energy in internal combustion cars. The engine coolant radiator and the exhaust line are the engine components that are used the most in the literature [11]. In literature, the TEG is placed in many locations at the exhaust system's conclusion, including after the exhaust catalyst and before the muffler and between the catalytic converter and the muffler's inlet [12–17]. The temperature of the engine cooling fluid, which is typically between 80 °C and 90 °C, is utilized as a heat absorber in TEG's automotive applications [18]. However, the high engine coolant temperature used for the cold side of TEMs has a detrimental impact on the TEMs' ability to produce power. In several studies, a liquid between 20 and 30 °C was used in the low-temperature heat exchanger. However, it does not seem possible to bring the engine coolant to this temperature due to restrictions such as operating the engine at regime temperature [19]. The development studies of TEG systems developed for waste heat recycling in internal combustion engine vehicles have been the subject of much research [20].

Vázquez et al. generated 125 W DC of electrical energy in TEG from the hot 600 °C exhaust gases of an internal combustion engine [21]. Dai et al. designed a TEG using liquid metal. The waste energy from the exhaust gases is transferred to the hot surface of the TEMs with the aid of liquid metal, and the electrical power of 120 W from 40 TEMs under an electrical load is generated [22]. Weng and Huang used theoretical simulation to investigate the effect of module number and coverage ratio on a TEG heat exchanger. They consequently observed that adding more modules to a TEG does not increase its net power output [17]. Hsu et al. conducted research on the designs of cold-side heat exchangers for TEGs. A maximum of 12.41 W is produced with 24 TEMs running at an average temperature differential of 30 °C using finned, air-cooled aluminum heat exchangers [23]. Durand et al. found that by positioning the TEG system after the exhaust manifold and exhaust catalyst, it achieved 100 W and 30 W of electrical power, respectively [24]. Kim et al. designed a three-layer TEG with a finned hot-side heat exchanger. They experimentally investigated the performance of TEG between 1000 and 2000 rpm in a diesel engine and obtained a TEG output power of 119 W with an efficiency of 2.8% [25]. Baatar et al. designed and operated a low-temperature TEG using the engine cooling fluid of light-duty automobiles and got an output power of approximately 28 W at idle engine speed [26]. Karri et al. designed a TEG utilizing an SUV vehicle's engine coolant. After accounting for the losses incurred when pumping the engine coolant, they discovered that their analyses saved about 2% of the gasoline [27]. The Nissan automobile company has developed a TEG that recycles the waste heat energy from a gasoline engine's exhaust gas through 72 TEMs. With the TEG developed, they produced 35.6 W of power, corresponding to approximately 0.9% of the heat flux that passes over the TEMs [28]. Love et al. designed a TEG consisting of five Bi_2Te_3 thermoelectric modules placed between stainless steel heat exchangers. They produced 3.8 W of power in tests performed at 1500 rpm of the engine under 70% engine load [29]. Gürbüz et al. investigated experimentally and theoretically the recovery by a newly developed TEG of energy lost by the hot exhaust gases of a propane-fueled SI engine. A maximum of 90.2 W of electrical power at 4500 rpm is obtained from a 2-cylinder, liquid-cooled SI engine with an efficiency of 3.02% [30].

When the previous studies are examined, the internal combustion engine waste heat recovery systems generally focus on the exhaust line and cooling fluid of the SI engine. In the present paper, unlike the previous studies, in a gas engine operated with propane fuel, the engine coolant was used as TEG's hot side heat exchanger (Ec_hex) fluid, and propane gas was used as TEG's cold side heat exchanger (P_hex) fluid. For this purpose, a two-layer TEG is designed. Between the Ec_hex and P_hex layers, 20 TEMs with dimensions of 30x30 mm are positioned. TEMs are electrically connected in series with each other. Experimental studies are performed at 8 different speeds in the range of 1500–5000 rpm on a 2-cylinder SI engine.

2. Material and Method

A two-layer TEG having rectangular geometry is designed, consisting of Ec_hex contacting the hot surface of the TEMs and P_hex contacting the cold surface of the TEMs. Both heat exchangers are designed as hollow, with dimensions (WxLxH) of 170 mm x 210 mm x 20 mm, and produced using aluminum welding from 2 mm thick aluminum sheet material. The heat exchangers are sized according to the reverse engineering principle, taking into account the surface area that the TEMs come into contact with. The surface area of TEG was sized to accommodate a total of 20 TEMs with dimensions of 30 x 30 mm in the thermoelectric layer. Considering the allowable hot and cold surface temperatures of TEMs, the designed TEG has a maximum power generation capacity of 100 W. The heights and thus the volumes of Ec_hex and P_hex were designed with an internal volume of 535 cm^3, taking into account the maximum coolant flow and maximum propane flow of the SI engine. In addition, a 3-layer sandwich structure was formed to ensure the contact of the TEMs with the heat exchanger surfaces, which is fixed to the heat exchangers and the TEM layer with 5 mm-thick lower and upper fixing plates and 4 bolts. A thin layer of thermal paste is used to minimize the contact resistance between Ec_hex contacting the hot surface of the TEMs and P_hex contacting the cold surface of the TEMs. The engine cooling fluid and propane gas are circulated counterclockwise with respect to each other through the heat exchangers by using nipple connectors and plastic hoses. Ec_hex and P_hex are positioned on top of each other, and a thermoelectric layer is created between them, between which 20 TEMs are placed. The exposed side surfaces of the Ec_hex and P_hex are covered with glass wool to prevent heat transfer to and from the atmosphere. While the cooling fluid entering the TEG is fed from the heating radiator outlet of the engine, propane gas is fed from a large 45 kg industrial propane cylinder at 1.2 bar pressure. The temperatures of the cooling fluid and propane at the inlet and outlet of the TEG are detected with K-type probe thermocouples. In addition, the temperatures affecting the hot and cold side surfaces of the TEMs are measured with K-type probe thermocouples placed at the midpoint of the Ec_hex and P_hex heat exchangers. The output parameters of the TEG are detected with an electronic load device assembled for the output of 20 TEMs connected in series with each other. The electrical load resistance applied to the output of TEG at each engine revolution is fixed at the value at which the maximum power output is provided by a series of tests. In TEG, the commercial product with the code TEG1-1263-4.3 produced by TECTEG is used, and its specifications is shown in Table 1.

The experimental studies are performed in a two-cylinder (in-line type) liquid-cooled, gas-fueled SI engine. Technical specifications for Lombardini LGW 523 MPI is given in Table 2. With a hydraulic dynamometer coupled to the output of the engine, it is provided to operate at different speeds and under load. The flow rates of the intake air and propane gas taken into the engine are measured using two mass flow meters (New-Flow TLF03A10111 and TSF03A10111, respectively). A 50/50 ethylene glycol/tap water blend is used as the cooling system of the engine and the hot-side fluid of TEG (inside Ec_hex). The experimental layout of an engine coolant energy recovery system is given in Fig.1.

Table 1. Specifications of TEMs (TEG1-1263-4.3) [3]

Temperature on the Hot/Cold side	300/30	°C
No-load voltage	10.7	V
Resistance to load	5.4	Ohms
Voltage at load output	5.3	V
Current at load output	1.0	A
Power to load	5.2	W
Heat pass through the module	≈ 115	W
Density of heat flow	≈ 13	W/cm^2

Table 2. Technical specifications of Lombardini LGW 523 MPI

Cylinder number and arrangement	2 cylinders (in-line)
Bore x Stroke (mm)	72 × 62
Total cylinder displacement (cm^3)	505
Compression ratio	10.7:1
Maximum speed (rpm)	5000
Maximum power (kW)	15 (@ 5000 rpm)
Maximum torque (Nm)	34 (@ 2150 rpm)
Colling system	Liquid cooled

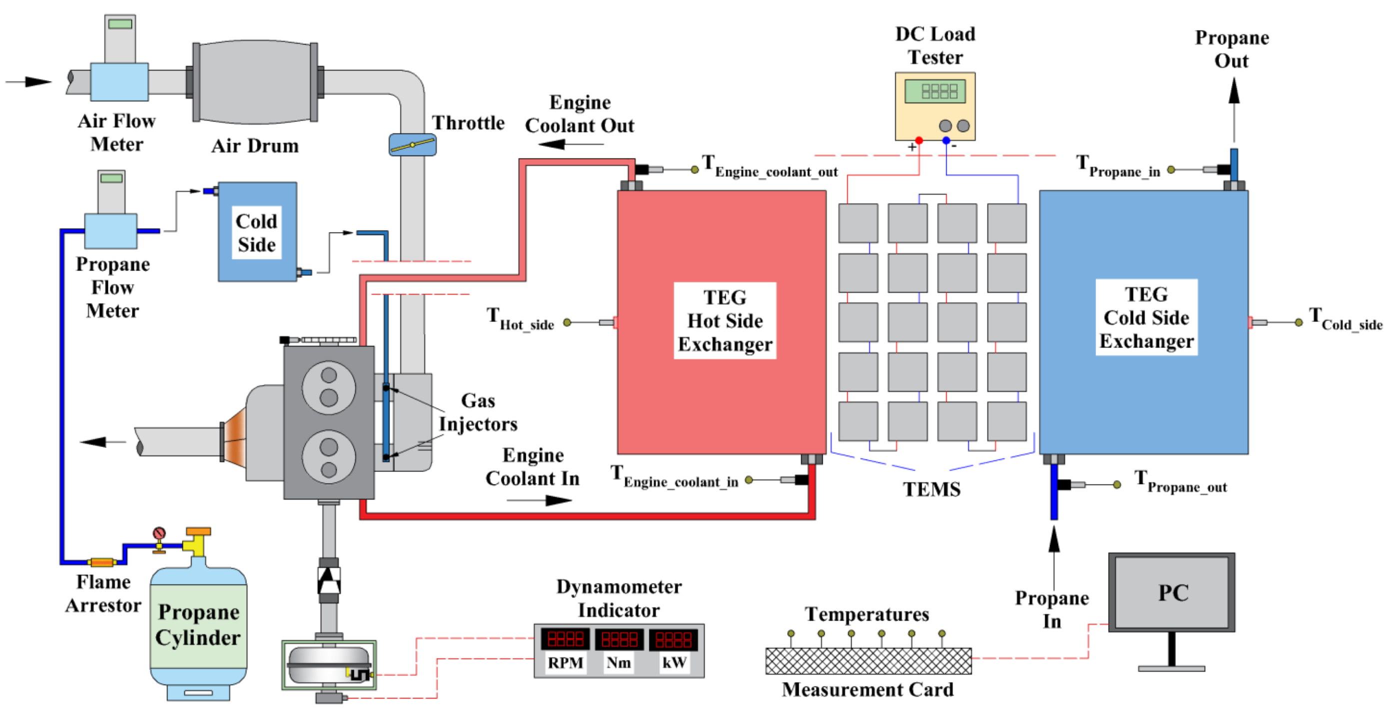

Fig.1. Experimental layout of an engine coolant energy recovery system

Experimental studies, the engine is operated in a constant 1/2 throttle position, and the air/fuel mixture is fixed around stoichiometric (0.97–1.05). At each engine speed, the propane-fueled SI engine is run for 5 min after increasing its operating temperature. The efficiency (TEG_efficiency) is calculated by Eq.1.

$$TEG\_efficiency = \left(\frac{TEG\_power}{\dot{m}_{ec} * c_{p\_ec} * (T_{ec\_in} - T_{ec\_out})}\right) * 100 \qquad (1)$$

Where TEG_power, $\dot{m}_{ec}$, and c_{p_ec} are the output power of TEG, the mass flow rate of engine cooling fluid, and the specific heat rate of engine cooling fluid, respectively. The engine cooling fluid's inlet and outlet temperatures into the TEG are T_{ec_in} and T_{ec_out}, respectively.

2.1. Uncertainty analysis

It is possible to calculate the uncertainty analysis of the experimental results using Eq.2 [31].

$$\Delta R = \left[\left(\frac{\partial R}{\partial x_1}\Delta x_1\right)^2 + \left(\frac{\partial R}{\partial x_2}\Delta x_2\right)^2 + \cdots + \left(\frac{\partial R}{\partial x_n}\Delta x_n\right)^2\right]^{1/2} \quad (2)$$

Uncertainty analysis was carried out at 5000 rpm, taking into account the accuracy of the instruments used in the experimental research in the measuring range. Table 3 provides the uncertainty analysis for a 5000 rpm engine speed.

Table 3. The uncertainty analysis for a 5000 rpm engine speed

Variable	Device	Accuracy	Parameters	5000 rpm	Error	[%]
BEP and BET	Go-Power System D-100	±1.5 %	BEP	4.64 kW	0.0567 kW	1.22%
Engine speed	MotecM4 and Pick-up	±6 rpm AR*	BSFC	0.569 kg/kWh	0.00406 g/kWh	0.71%
Propane flow rate	New-flow TLF03A10111	±1.5% FS ±0.33%**	$\dot{m}_p$	0.421 kg.min^{-1}	0.001 kg.min^{-1}	0.24%
Temperature	K type thermocouple	±0.75 %	T_{ec}	82.43 °C	0.654 °C	0.79%
	DAQ card	±0.4 %	T_p	57.7 °C	0.443 °C	0.77%
Volt	UNI-T UT33A	±0.5 %	ΔT	28.03 °C	0.209 °C	0.74%
Ampere	Multimeter	±2 %	TEG_power	3.1 W	0.018 W	0.58%

* AR: All range, FS: Full scale, **Accuracy of device in measurement range

3. Discussion and Findings

The use of TEGs for waste heat recycling of ICE cars in real operating conditions is becoming widespread. Many commercial companies, such as GM and BMW, have already moved into the TEG development phase as a final product. Successful studies using TEG have converted exhaust waste heat energy into electrical energy with a conversion efficiency of approximately 5–10% [32-36]. Moreover, a team from Gentherm, which develops comfort systems for automotive companies such as BMW, Ford, and Faurecia, carried out performance tests with the integration of TEG on BMW X6 and Lincoln MKT brand and model passenger cars [37]. Similarly, the LGW 523 MPI brand and model SI engine used in this study is currently used in the Microcar MC1 brand and model small passenger car. Therefore, the results of the paper have the potential to be used directly in the automobile industry. Fig.8 depicts the changing of engine performance parameters with engine speed. The engine produced a maximum braking engine torque (BET) of 22 Nm at 2000 rpm with a 1/2 throttle opening, and at 5000 rpm the BET decreased to 9 Nm. The brake engine power (BEP) is approximately 5.5 kW in the range of 3000–4000 rpm, increasing to a maximum BEP of 5.51 kW at 4000 rpm engine speed. While the brake-specific fuel consumption (BSFC) is 0.297 kg/kWh at 1500 rpm, it increased with engine speed and reached 0.569 kg/kWh at 5000 rpm.

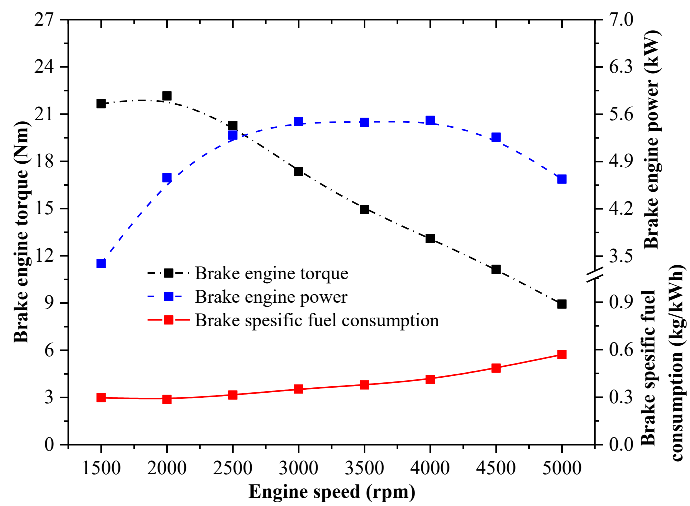

Fig.2. Changing of engine performance parameters versus engine speed

The variations of mass flow rates of engine cooling fluid and propane versus engine speeds is illustrated in Fig.9. In the range of 1500–5000 rpm, at the TEG's inlet, the rates of mass flow of propane ($\dot{m}_p$) and engine cooling fluid ($\dot{m}_{ec}$) vary between 0.183 and 0.421 kg.min^{-1} and 0.0168 and 0.0441 kg.min^{-1}, respectively. In addition, both mass flow rates increased based on the increase in engine speed. That is, depending on the rise in engine speed, the mass flow rates of the engine cooling fluid and propane into the TEG increased.

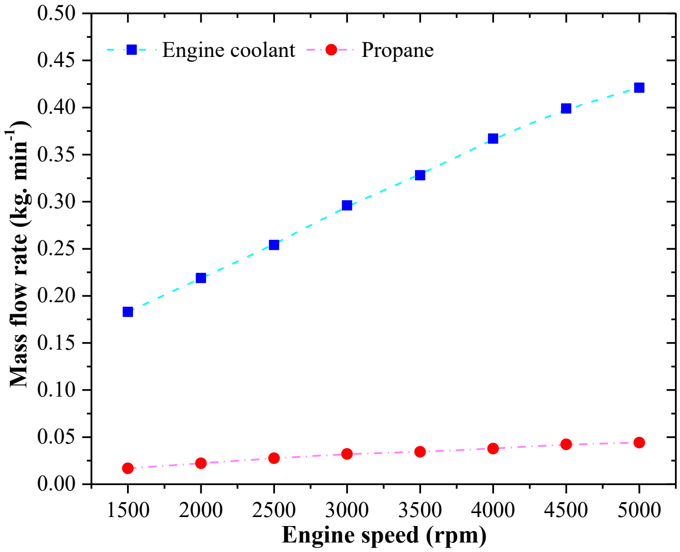

Fig.3. Variation of mass flow rates of engine cooling fluid and propane versus engine speed

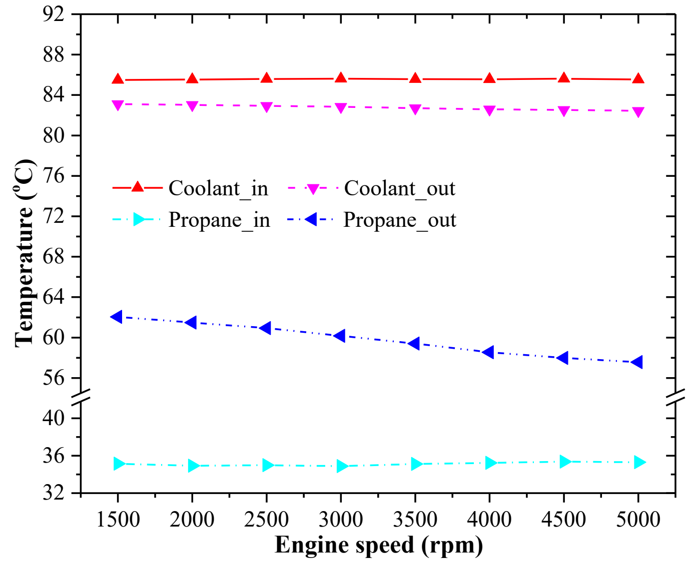

Fig. 4. Variation of engine cooling fluid and propane into TEG inlet and outlet temperatures relative to engine speed

Fig. 4 depicts the variation of temperatures at the inlet and outlet of engine cooling fluid and propane into the TEG versus engine speed. The temperature of the engine coolant fed to the TEG from the heating radiator output line of the engine remained constant at approximately 85.5 °C between 1500 and 5000 rpm. In general, the engine cooling fluid temperature (T_{ec}) at the outlet of TEG decreased for all engine speeds due to the heat transferred to the propane gas by the occurring heat flow across the TEMs. However, the engine cooling fluid temperature at the TEG output slightly decreased with increasing engine speed due to the rise in the propane gas flow rate taken into the TEG depending on the increasing engine speed. On the other hand, the temperature of the propane gas fed into the TEG remained constant at approximately 35.2 °C in the range of 1500–5000 rpm. However, due to the increase in the mass of propane fed into the TEG with the increased engine speed, the outlet temperature of the propane gas (T_p) from the TEG decreased remarkably. While the exit temperature of propane gas from TEG is 62 °C at 1500 rpm, it declines to 57.6 °C at 5000 rpm. A positive result of this finding is that, with the rise in engine speed, the difference in temperature affecting the hot and cold side surfaces of the TEMs increases (see Fig.5). Because increasing the engine speed causes the outlet temperature of the propane from the TEG to decrease more than the outlet temperature of the engine coolant.

The variation of the temperature at the surface of Ec_hex and P_hex versus engine speed is illustrated in Fig.5. As seen in Fig.5, the temperature at the surface of the Ec_hex in contact with the hot side surface of the TEMs increases from 83.5 °C to 85.4 °C with the engine speed. On the other hand, the temperature of P_hex's surface in contact with the TEMs' cold side surface decreases from 60.2 °C to 57.4 °C. When the engine speed is raised from 1500 rpm to 5000 rpm, the increase in Ec_hex is about 1.9 °C, while the decrease in P_hex is about 2.9 °C. This result contributed significantly to the increase in the temperature difference (ΔT) between the TEMs' hot and cold surfaces as engine speed increased. While the difference in temperature (ΔT) between the ceramic layer surfaces in contact with the heat exchanger of the TEMs is 23.3 °C at 1500 rpm, the temperature difference (ΔT) increased to 28.1 °C at 5000 rpm.

According to these results, the increase in temperature difference (ΔT) acting on the surfaces of the TEMs despite constant engine coolant and propane gas inlet temperatures in the range of 1500–5000 rpm depends on the increase in mass flow rates of the engine cooling fluid and propane gas. In this case, it is expected that the no-load/open circuit voltage of TEG, the voltage and current under load, and finally TEG_power will increase with engine speed (see Fig.6, Fig.7, and Fig.8).

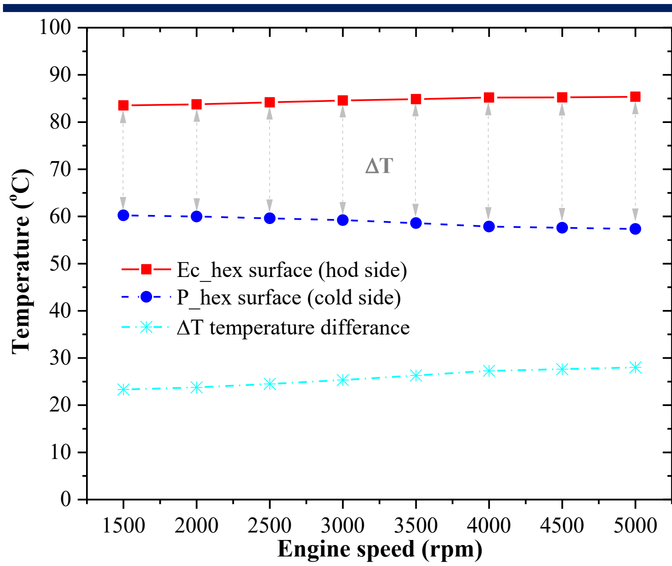

Fig.5. Variation of surface temperatures of Ec_hex and P_hex versus engine speed

The open circuit voltage of TEG (20 TEM series) with engine speed is indicated in Fig. 6. As shown in Fig.6, the no-load voltage of TEG increased as the ΔT acting on the hot and cold surfaces of the TEMs increased with engine speed (see Fig.5). While the no-load voltage is 16.9 V at 1500 rpm, it increased to 25.6 V at 1500 rpm. While the rate of increase in TEG no-load voltage is rapid up to 4000 rpm, it then slows depending on the ΔT temperature difference after 4000 rpm.

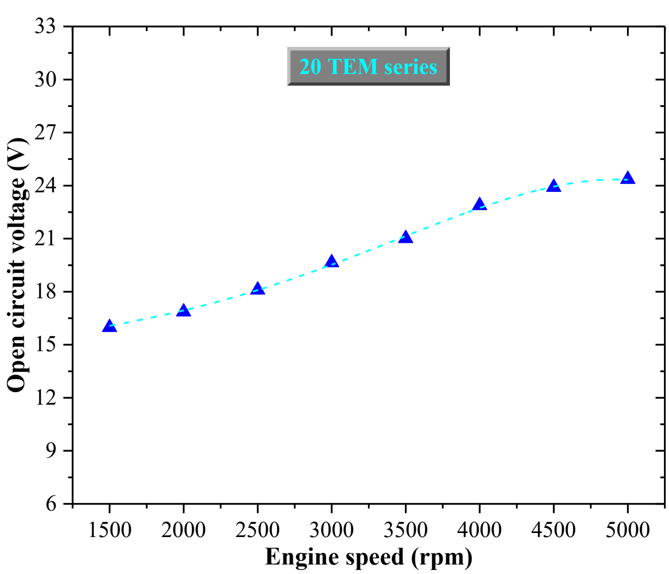

Fig.6. No-load voltage of TEG (20 TEM series) versus engine speed

Fig.7 depicts the variation of load voltage and load current of the TEG versus engine speed. In the experiments, the load voltage and current are measured with an electronic load device fixed to the output of 20 series-connected TEM modules. The applied load voltage is chosen for the optimum value that gives the highest power. The applied load voltage between 1500 and 5000 rpm changed in the range of 82.2–84.1 ohms. TEG's load voltage and load current increase with motor speed. TEG's load voltage rises from 9.1 V at 1500 rpm to 14.1 V at 5000 rpm. In contrast, the load current of TEG increases from 0.137 A at 1500 rpm to 0.214 A at 5000 rpm. It should be noted that the temperature difference between the surfaces of the TEMs characterized the change curves of the load voltage and load current of the TEG related to increasing engine speed.

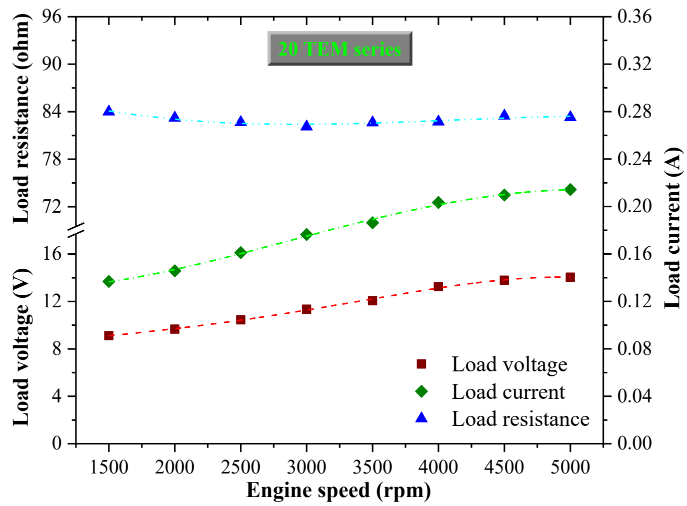

Fig.7. Variation of load resistance, load voltage, and load current of TEG versus engine speed

The change of TEG_power versus engine speed is given in Fig.8. Firstly, it is seen that the TEG_power increases depending on increasing engine speed. The increase in TEG_power with engine speed depends on the increase in the difference in temperature (ΔT) between the hot and cold side surfaces of the TEM, which is the main factor for TEM technology. The minimum TEG_power is obtained with 1.25 W at 1500 rpm, while the maximum TEG_power is obtained with 3.01 W at 5000 rpm. While TEG_power increased rapidly up to 4000 rpm, the increase rate slowed down after 4000 rpm. The main reason for the slowdown after 4000 rpm can be depicted by the increase in heat transfer losses from Ec_hex surfaces to the environment, depending on the rise in the rate of mass flow of the hot-side fluid (engine cooling fluid).

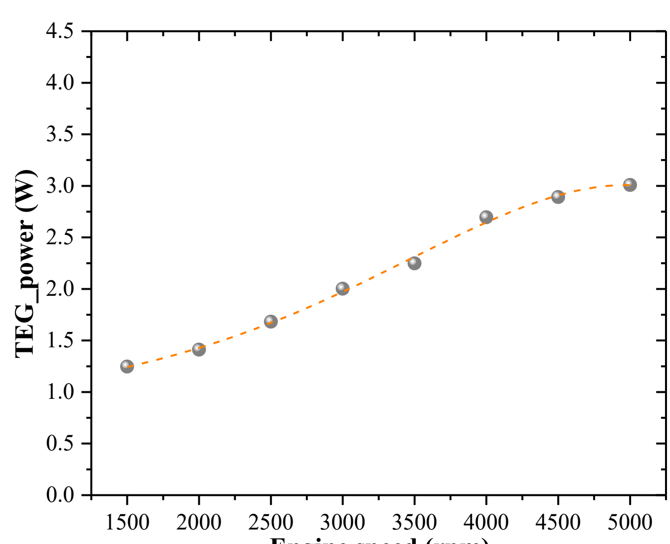

Fig.8. Variation of TEG_power versus engine speed

Fig. 9 illustrates the variation in TEG_efficiency with engine speed. TEG_efficiency is at its highest value of 3.1% at 1500 rpm, decreases slightly with engine speed (2.8% at 2000 rpm), and finally remains constant at around 2.75%, despite small changes in the range of 2500–5000 rpm. The main reason TEG_efficiency is maxed out at 1500 rpm is that the engine cooling fluid flow rate is lower at lower engine speeds than at higher engine speeds. The heat losses from Ec_hex to the atmosphere increased with the increase in the engine cooling fluid flow rate taken into the TEG. Because the high engine coolant mass flow rate caused the Ec_hex volume to fill more and the hot fluid to come closer to the surfaces. However, the 2.75% TEG_efficiency obtained at high engine speeds is acceptable when compared with the literature. Gürbüz et al. stated that the TEG efficiency changed between 1-3.1% in the range of 1500–5000 rpm with the TEG they developed for a gas-fueled SI engine [30].

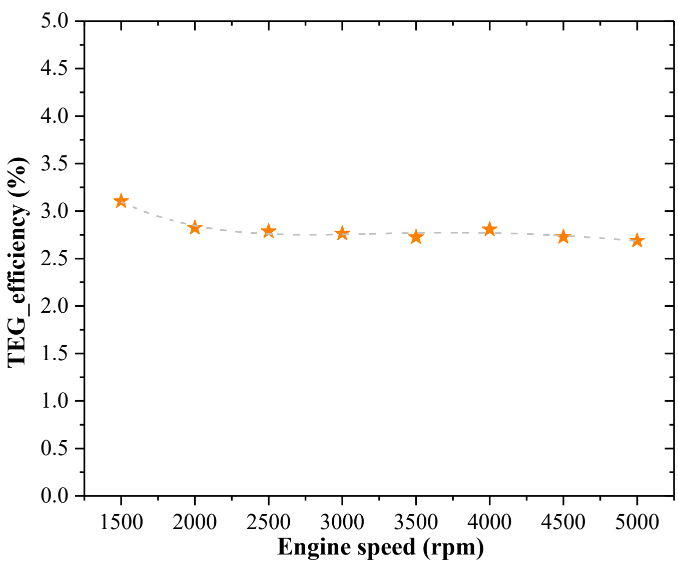

Fig.9. TEG efficiency variation with engine speed

TEG's contribution to the charging system with engine speed is illustrated in Fig.10. The test engine has an internal alternator consisting of a circular permanent magnet placed in the inner bowl of the engine flywheel and a stationary stator winding placed inside this magnet. The permanent magnet placed in the inner bowl of the engine flywheel is rotated at the same speed as the engine. The internal alternator produces a maximum current of 30 amps at a voltage of 12.5 volts and increases with engine speed. The power produced by TEG corresponds to approximately 1.1% of the power of the engine charging system at other engine speeds except for 1500 rpm. The contribution rate of TEG to the charging system at 1500 rpm is approximately 1.26%.

In addition to the contribution of TEG to the engine's charging system, there will be no need for an additional evaporator for the preheating (evaporation) of the propane gas fed to the engine for the gas-fueled SI engine. Thus, the cost of additional equipment is also reduced. In addition, with TEG, additional power is obtained in the gas-fueled SI engine without any reduction in engine power, thus providing fuel savings.

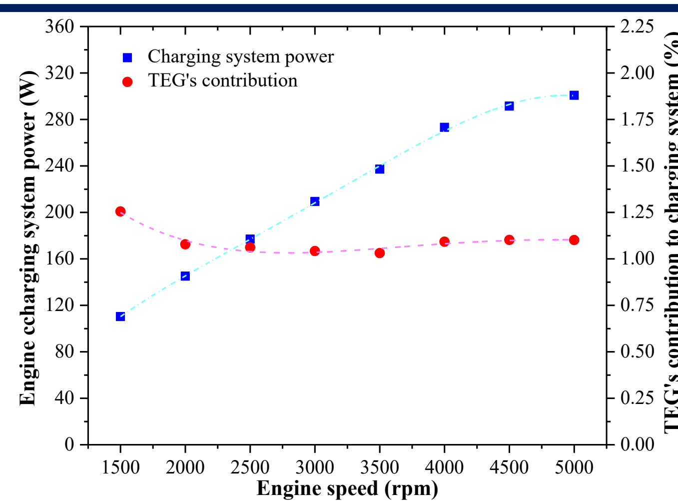

Fig.10. TEG's contribution to the charging system versus engine speed

4. Conclusions

The results of the paper, in which the conversion of heat energy lost to the cooling fluid of a propane-fueled, water-cooled, 2-cylinder SI engine into electrical energy with the help of a TEG is examined, are summarized as follows:

- The outlet temperatures of the engine coolant taken to the TEG at a temperature of approximately 85.5 °C at all engine speeds varied between 82.4 and 83.1 °C with the engine speed. The exit temperature of the propane gas entering the TEG at a temperature of approximately 35.1 °C changed between 57.7 and 62 °C with engine speed. While the outlet temperature of the engine cooling fluid from the TEG increased with the engine speed, the exit temperature of the propane gas from the TEG decreased. Thus, the difference in temperature between the surfaces of the TEMs increased with engine speed.
- The open circuit voltage of TEG, which is approximately 16.9 volts at 1500 rpm, increased to 25.6 volts at 5000 rpm, with the effect of increasing the temperature difference. By increasing the engine speed from 1500 rpm to 5000 rpm, the load current of the TEM series increased from 0.137 amps to 0.214 amps, and the load voltage increased from 9.1 volts to 14.1 volts. The load resistance applied to the TEG output changed in the range of 82.2–84.1 ohms with the engine speed. With TEG, a maximum output power of 3.01 W was obtained at 5000 rpm with an efficiency of 2.7%, while a maximum efficiency of 3.1% was obtained with an output power of 1.25 W at 1500 rpm. Furthermore, the contribution rate of TEG output power to the power of the engine charging system is approximately 1.1% at other engine speeds excluding 1500 rpm (1.26%).

Credit of Interest Statement

The authors declare that there is no conflict of interest in the paper.

CRediT Author Statement

Habib GÜRBÜZ: Supervision, Investigation, Methodology, Writing & Editing, Visualization
Hüsameddin Akçay: Experimental setup, Data collection, Writing-Original Draft, Visualization
Beyza ÖZTOP: Experimental setup, Data collection, Writing-Original Draft, Visualization

References

[1] Anastasiou A., Marietta P. Sustainable Development at the Frames of the Strategy "Europe 2020". Theoretical Economics Letters. 2020;10(03):443.

[2] In BD., Kim H-ik, Son JW, Lee K-Hyung. The study of a thermoelectric generator with various thermal conditions of exhaust gas from a diesel engine. Int J Heat Mass Transf. 2015; 86:667-680.

[3] Gürbüz H, Akçay H. Experimental investigation of an improved exhaust recovery system for liquid petroleum gas fueled spark ignition engine. Therm Sci. 2015;19(6):2049-2064.

[4] Zabrocki CK. Continuum Theory and Modeling of Thermoelectric Elements; Goupil, C., Ed. 2016:84-90, ISBN: 978-3-527-41337-9.

[5] Yu C, Chau KT. Thermoelectric automotive waste heat energy recovery using maximum power point tracking. Energy Convers Manag. 2009;50(6):1506-1512.

[6] Saidur R, Rahim NA, Ping HW, Jahirul, MI, Mekhilef S, Masjuki HH. Energy and emission analysis for industrial motors in Malaysia. Energy Policy, 2009;37(9):3650-3658.

[7] Huang K, Yan Y, Li B, Li Y, Li K, Li J. A novel design of thermoelectric generator for automotive waste heat recovery. Automotive Innovation. 2018; 1:54-61.

[8] Nader WB. Thermoelectric generator optimization for hybrid electric vehicles. Appl Therm Eng. 2020; 167:114761.

[9] Montecucco A, Siviter J, Knox AR. The effect of temperature mismatch on thermoelectric generators electrically connected in series and parallel. Appl Energy. 2014; 123:47-54.

[10] Siddiqui FM, Maurya VK. Study of TEG When Connected in Series and Parallel Combinations Along With a DC-DC Converter. Vivechan Int J Res. 2017;8(1):76-86.

[11] Wang Y, Dai C, Wang S. Theoretical analysis of a thermoelectric generator using exhaust gas of vehicles as heat source. App Energy, 2013;112:1171-1180.

[12] Al-Merbati AS, Yilbas BS, Sahin AZ. A model study for cyclic thermal loading and thermal performance of a thermoelectric generator. Int J Energy Res. 2014;38(10): 1351-1360.

[13] Sharma S, Dwivedi VK, Pandit SN. Exergy analysis of single-stage and multi stage thermoelectric cooler. Int J Energy Res. 2014;38(2):213-222.

[14] Bélanger S, Gosselin L. Multi-objective genetic algorithm optimization of thermoelectric heat exchanger for waste heat recovery. Int J Energy Res. 2012;36(5):632-642.

[15] Sahin AZ, Yilbas BS. The influence of operating and device parameters on the maximum efficiency and the maximum output power of thermoelectric generator. Int J Energy Res. 2012;36(1):111-119.

[16] Hwang, HK, Seo JW, Seo WS, Lim YS, Park K. Thermoelectric properties of P-doped and V-doped Fe_2O_3 for renewable energy conversion. Int J Energy Res, 201438(2), 241-248.

[17] Weng CC, Huang MJ. A simulation study of automotive waste heat recovery using a thermoelectric power generator. Int J Therm Sci. 2013; 71:302-309.

[18] Fernández-Yáñez P, Gómez A, García-Contreras R, Armas O. Evaluating thermoelectric modules in diesel exhaust systems: potential under urban and extra-urban driving conditions. J Clean Prod, 2018;182:1070-1079.

[19] Ezzitouni S, Fernández-Yáñez P, Sánchez L, Armas O. Global energy balance in a diesel engine with a thermoelectric generator. Appl Energy. 2020; 269:115139.

[20] Orr B, Akbarzadeh A, Mochizuki M, Singh R. A review of car waste heat recovery systems utilising thermoelectric generators and heat pipes. Appl Therm Eng. 2016; 101:490-495.

[21] Vázquez J, Sanz-Bobi MA, Palacios R, Arenas A. State of the art of thermoelectric generators based on heat recovered from the exhaust gases of automobiles. In Proc. 7th European workshop on thermoelectrics (No. 17). October 2002.

[22] Dai D, Zhou Y, Liu J. Liquid metal based thermoelectric generation system for waste heat recovery. J Renew Energy. 2011;36(12):3530-3536.

[23] Hsu CT, Huang GY, Chu HS, Yu B, Yao DJ. Experiments and simulations on low-temperature waste heat harvesting system by thermoelectric power generators. Appl Energy, 2011;88(4):1291-1297.

[24] Durand T, Eggenschwiler PD, Tang Y, Liao Y, Landmann D. Potential of energy recuperation in the exhaust gas of state of the art light duty vehicles with thermoelectric elements. Fuel. 2018; 224:271-279.

[25] Kim TY, Negash AA, Cho G. Waste heat recovery of a diesel engine using a thermoelectric generator equipped with customized thermoelectric modules. Energy Convers Manag. 2016; 124:280-286.

[26] Baatar N, Kim S. A thermoelectric generator replacing radiator for internal combustion engine vehicles. TELKOMNIKA (Telecommunication Computing Electronics and Control), 2011;9(3):523-530.

[27] Karri MA, Thacher EF, Helenbrook BT. Exhaust energy conversion by thermoelectric generator: Two case studies. Energy Convers Manag. 2011;52(3):1596-1611.

[28] Ikoma K, Munekiyo M, Furuya K, Kobayashi MAKM, Izumi TAIT, Shinohara KASK. Thermoelectric module and generator for gasoline engine vehicles. In Seventeenth International Conference on Thermoelectrics. Proceedings ICT98 (Cat. No. 98TH8365) IEEE, May 1998:464-467.

[29] Love ND, Szybist JP, Sluder CS. Effect of heat exchanger material and fouling on thermoelectric exhaust heat recovery. Appl energy, 2012;89(1):322-328.

[30] Gürbüz H, Akçay H, Topalcı Ü. Experimental investigation of a novel thermoelectric generator design for exhaust waste heat recovery in a gas-fueled SI engine. Appl Therm Eng. 2022; 216:119122.

[31] Akçay İH, Gürbüz H, Akçay H, Aldemir M. An investigation of euro diesel-hydrogen dual-fuel combustion at different speeds in a small turbojet engine. Aircraft Eng Aero Technol 2021;93(4):701–710.

[32] Liang X, Sun X, Tian H, Shu G, Wang Y, Wang X. Comparison and parameter optimization of a two-stage thermoelectric generator using high temperature exhaust of internal combustion engine. Appl Energy 2014;130:190–199.

[33] Weng CC, Huang MJ. A simulation study of automotive waste heat

recovery using a thermoelectric power generator. Int J Therm Sci 2013;71:302–309.

[34] Armstead JR, Miers SA. Review of waste heat recovery mechanisms for internal combustion engines. J Therm Sci Eng Appl 2014;6(1).

[35] Mazar B. State of the art prototype vehicle with a thermoelectric generator. In 3rd Thermoelectrics Applications Workshop March 2012;1-13.

[36] Crane DT. Thermoelectric Waste Heat Recovery Program for Passenger Vehicles. US Department Energy Efficiency & Renewable Energy (EERE) 2012:114-121.

[37] Crane D, LaGrandeur J, Jovovic V, Ranalli M, Adldinger M, Poliquin E, Dean J, Kossakovski D, Mazar B, Maranville C. TEG on-vehicle performance and model validation and what it means for further TEG development. J Electron Mater 2013;42, 1582-1591.